Mass-Analyzed Threshold Ionization of the *trans*-1-Naphthol−Water Complex: Assignment of Vibrational Modes, Ionization Energy, and Binding Energy†

J. E. Braun and H. J. Neusser*

Institut für Physikalische und Theoretische Chemie, Technische Universität München, Lichtenbergstr. 4, D - 85748 Garching, Germany

Received: April 21, 2003; In Final Form: July 23, 2003

Naphthol is a prototype example for the enhancement of the molecule-to-solvent proton transfer after electronic excitation. In this work, we investigate the influence of water molecules attached to naphthol on the spectroscopic properties of the neutral excited-state S_1 and the ionic state. In addition to $S_1 \leftarrow S_0$ spectra, we present mass-analyzed threshold ionization (MATI) spectra for 1-naphthol and for the first time of the 1-naphthol·H_2O complex displaying a rich variety of intra- and intermolecular vibrational bands. The comparison of ionic spectra measured via different intermediate states allows us to assign various vibrational modes in the monomer and the 1-naphthol·H_2O cluster assuming a $\Delta\nu = 0$ propensity rule. Assignment is also based on the energies and atomic displacement patterns of vibrations calculated from ab initio theory.

Introduction

Electronically excited naphthol (NP) has a higher probability for donation of a proton from the OH group to a surrounding solvent than ground-state NP,[1,2] that is, the acidity of NP is enhanced after electronic excitation. There exist two possible isomers *1-naphthol* (1NP) and *2-naphthol* (2NP), depending on the position of the OH group. The enhancement of acidity in the S_1 state is strongest for the 1NP. Here the pK_A value of the molecule in the ground state is 9.4 while the corresponding value in the S_1 is only 0.5. The mechanism of the proton transfer from the NP molecule to the solvent leading to an enhancement of the acidity in the excited state has been investigated in a series of publications in the liquid phase[1−4] and more recently in clusters.[5−15]

Several spectroscopic experiments have been carried out to understand the mechanism of molecule−solvent interactions. In the ground and the first excited electronic state ^1L_b (S_1, A′), NP is planar and has C_S symmetry. NP has 35 in-plane modes with symmetry a′ and 16 out-of-plane modes with symmetry a″. Both transitions A′←A′ and A″←A′ are symmetry-allowed, resulting in a relatively dense band structure in the excitation spectra. Hollas and Thakur analyzed the rotational contour of absorption spectra of 1NP taken in the gas phase at room temperature.[16] Then, laser-induced fluorescence (LIF) and resonance-enhanced multiphoton ionization (REMPI) spectra of isolated 1NP were measured in a cold molecular beam.[5] Evidence for the existence of two rotational conformers (rotamers) with a different orientation of the OH group, whose absorption maxima differ by 274 cm^{-1}, was first found at room temperature[17] and later corroborated by fluorescence excitation spectra in the cooled supersonic molecular beam and by zero kinetic electron energy−pulsed field ionization (ZEKE−PFI).[18−20] The energy of the trans configuration in the ground state is 220 ± 50 cm^{-1} lower than the ground state of the cis rotamer.[18] The rate constants for the proton separation were determined in solution,[3,21] in Ar matrix,[22] and in femtosecond pump/probe experiments with clusters of NP with water, NH_3, and piperidine.[11]

In the present work, additional information on the S_1 electronic state is obtained from ionic spectra measured via different intermediate vibronic states in S_1 with the technique of mass-analyzed threshold ionization (MATI) after resonance-enhanced two-photon ionization. Furthermore, using this technique, vibrational spectra of the cationic ground-state $\tilde{X}$ of the *trans*-1NP·H_2O cluster are presented. Comparing these spectra with the $S_1 \leftarrow S_0$ REMPI spectra of the monomer and cluster and ab initio results, most of the vibrational bands in the neutral S_1 and ionic $\tilde{X}$ states of monomer and cluster were assigned properly, leading to new insights into the intermolecular interactions.

Experimental Section

The experimental setup used was described in detail elsewhere.[23,24] Briefly, a gas mixture of 1NP vapor which is vaporized inside a heated (110 °C) valve and seeded in a mixture of Ne (≈3 bar) and ≈25 mbar H_2O is expanded through a pulsed (10 or 25 Hz) nozzle supersonically into the vacuum, producing a cold molecular beam of 1NP and clusters of 1NP with water. Two dye lasers (FL 3002 and LPD 3000; Lambda Physik) pumped synchronously by a XeCl excimer laser (EMG 1003i, Lambda Physik) and yielding ≈10 ns light pulses with a bandwidth of ≈0.3 cm^{-1} are used for the excitation. The two counter propagating laser beams intersect the skimmed supersonic molecular beam perpendicularly 15 cm downstream from the nozzle orifice. The light pulses overlap in time and space in the center of the ion optics of a linear reflecting time-of-flight mass spectrometer.[25,26] The direct ionization (REMPI) or excitation to high Rydberg levels (MATI) of 1NP or 1NP·H_2O clusters is achieved by a resonantly enhanced two-photon two-color process. In the MATI process, promptly produced cations originating from a direct two-photon ionization process (prompt ionization) of molecules are separated from molecules in long-lived high Rydberg states. This is performed by a delayed pulsed weak electric field (separation field, ≈0.6 V/cm), which is applied to the first zone (30-mm wide) of the ion optics, in

† Part of the special issue "Charles S. Parmenter Festschrift".

* Address correspondence to this author.

10.1021/jp0304677 CCC: $25.00
Published on Web 09/25/2003

such a way that the prompt ions are decelerated. The separation field is switched on about 100 ns after the occurrence of the two laser pulses.[24] Within several μs, the neutral high Rydberg molecules drift into a second zone (20-mm wide) where no electric field is present at that time. An ionization field of 500 V/cm is switched on 28 μs after the occurrence of the two exciting/ionizing laser pulses and ionizes the high Rydberg molecules. The resulting threshold ions are accelerated toward the ion reflector by this electric field and then reflected toward the multichannel plates. At this time, the prompt ions have not yet arrived at the second zone so that they are not accelerated. Threshold ion and REMPI spectra are recorded mass selectively with a gated integrator/microcomputer system running under a LabView environment.

Ab Initio Calculations

All ab initio calculations in this work were performed with the Gaussian 94 package.[27] We determined the atom positions (geometry) and also the normal-mode frequencies of the *trans*-1NP monomer in the neutral ground-state S_0, the first excited electronic state S_1, and the cationic ground-state $\tilde{X}$, respectively. In a first approximation, because of a large Franck−Condon factor, a certain (vibrational) excitation is preserved during a transition from one electronic state to another when the molecular potential does not change too much. Otherwise (as was observed for the $S_1 \leftarrow S_0$ transition in 1NP[12]) one normal mode, for example, in the S_0 has no direct counterpart in S_1 but is a linear combination of normal modes in the S_1 and vice versa. We computed the overlap of the calculated normal mode displacement patterns of the molecule or cluster in its different electronic states S_0, S_1, and $\tilde{X}$. A normal mode ν'' with quantum number ν'' in an initial electronic state can be described as a linear combination of several normal modes ν' in a final electronic state, neglecting possible geometrical distortions of the molecule: $|\nu_j''=1\rangle = \Sigma_i a_i |\nu_i'=1\rangle$. If more than one of the coefficients a_i are large, there is significant coordinate (Duschinsky) rotation.[28]

Calculating the coefficients a_i for the excitation of the respective vibrations during an electronic transition, for example, $\tilde{X} \leftarrow S_1$, was helpful for the proper assignment of the bands in both electronic states. On the basis of the $S_1 \leftarrow S_0$ and $\tilde{X} \leftarrow S_1$ spectra of this work and the $S_1 \rightarrow S_0$ emission spectra from the literature,[12] we were able to assign most of the vibrations unambiguously.

The *trans*-1NP·H_2O cluster geometries in the different electronic states were calculated in three iterations: (i) In the first step, the geometries of the molecules *trans*-1NP and H_2O were calculated separately. (ii) Next, the cluster was assumed to be composed of the two rigid molecular moieties and only the intermolecular degrees of freedom were varied. (iii) Finally, in the most time-consuming step, the whole cluster geometry was optimized without any restrictions in the degrees of freedom. This was possible because the starting geometry for the third step was already near the optimum. The precision for the calculated geometries and frequencies in the S_0 states were restricted to the Hartree−Fock (HF) level and for the S_1 states to single configuration interaction (CIS). In all cases, an enhanced correlation consistent (cc-pVDZ) basis set was used. This basis set was additionally extended at the C and O atoms by the diffuse functions of the 6-31+G basis set ("cc-pVDZ+"). The calculated vibrational frequencies were about 10− 20% too high, which was corrected by comparing the calculated frequencies with the measured frequencies in the REMPI and MATI spectra of this work and fluorescence and IR spectra from the literature.[12,17,20,29]

TABLE 1: Vibrational Modes in the Neutral S_1 and Ionic $\tilde{X}$ state of *trans*-1-Naphthol and the *trans*-1-Naphthol·H_2O Cluster Found in the $S1 \leftarrow S_0$ REMPI Spectrum, the $\tilde{X} \leftarrow S_1$ MATI Spectrum, and by ab Initio Calculations[a]

	intermediate state S_1				cation $\tilde{X}$			
	monomer		cluster		monomer		cluster	
mode	exptl	theor	exptl	theor	exptl	theor	exptl	theor
	31456		31313.5		62640		59130	
β_{oop}			30	26.7				51.3
β_{ip}			56	52				77
s				94			190	173
49	209	200	209	208	237	231		234
35	275	273	293	294	282	296	327	319
34	411	443	402	450	445	454	459	464
46	415	390	495	489			510	509
33	454	449	456	457	460	465	490	469
32	492	497	502	508	510	525	532	540
31	546	530	549	540	550	574		579
45		443		578		594	651	666
30	666	676	671	685	700	707	714	709
43		549		698	730	727		769
42	707	685	716	707		773		816
41	716	699		719		806		885

[a] The energy values are given in [cm^{-1}] and compared to the theoretical results. Intermolecular modes of the cluster are designated by greek letters.

TABLE 2: Theoretical and Experimental Ionization Energies of 1-Naphthol and 1-Naphthol·H_2O

	ionization energies [cm^{-1}]		
	experiment	theory	deviation
1-naphthol	62640	64839	2192 (3.4%)
1-naphthol·H_2O	59130	61323	2194 (3.7%)

TABLE 3: Theoretical and Experimental Binding Energies of 1-Naphthol·H_2O in Its Neutral Ground State S_0 and the Cationic Ground State $\tilde{X}$

electronic state of 1-naphthol·H_2O	binding energy [cm^{-1}]		
	experiment	theory	deviation
S_0	2035 ± 69	1619	416 (25.7%)
$\tilde{X}$	5547 ± 75	4932	621 (11.2%)

Throughout the work for the normal modes, the Mulliken convention[30] is used (the *x*-axis is perpendicular to the 1NP molecular plane, the *z*-axis is parallel to the long molecular axis). The numbering convention is to start with the highest frequency a′ mode as no. 1 and enumerate modes of this symmetry in the order of decreasing frequencies. The a″ modes start at no. 36 and are also numbered in the order of decreasing frequencies. The numbering was done individually for each electronic state. Therefore, vibrations of equal numbers do not necessarily have similar displacement patterns. All calculated vibrational frequencies of the *trans*-1NP and the *trans*-1NP·H_2O cluster in the different electronic states S_0, S_1, and $\tilde{X}$ are listed in Table 1, together with the experimental values and the band assignments found in this work.

For the calculation of the total energies of the molecule and the cluster in its different electronic states, a Møller−Plesset (MP2) procedure was employed, using several basis sets 6-311G(d,p), 6-311G(df,p), 6-311+G(d,p), and 6-311G(2df,-2p). The results are presented in Tables 2 and 3 and compared with experimental results for the ionization energies (IE).

Experimental Results and Discussion

trans-1-Naphthol Monomer. The $S_1 \leftarrow S_0$ intermediate state spectrum of bare 1NP, recorded over a range of 800 cm^{-1} by

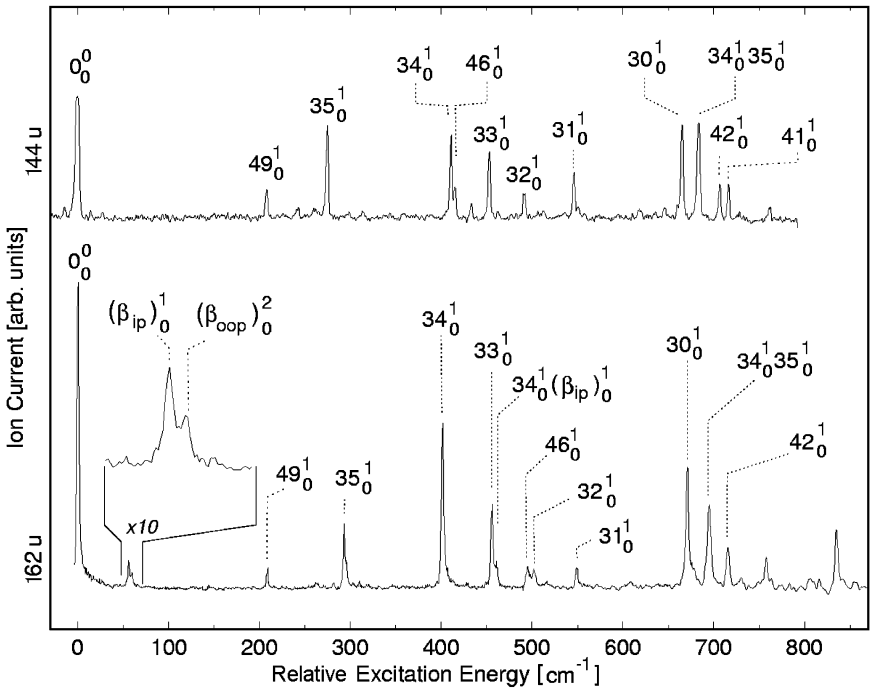

Figure 1. $S_1 \leftarrow S_0$ REMPI spectra of *trans*-1-naphthol (upper trace) and the *trans*-1-naphthol·H_2O cluster (lower trace). Both spectra are displayed on a common relative excitation energy scale. The position of the 0^0_0 origins are 31456 cm^{-1} for 1-naphthol and 31313.5 cm^{-1} for 1-naphthol·H_2O. For explanations, see text.

resonantly enhanced two-photon two-color ionization (REMPI), is shown in the upper trace of Figure 1. We assigned the $S_1 \leftarrow S_0$, 0^0_0 origin to the trans rotamer with an energy of 31456 cm^{-1}, according to the values found in the literature (31457.6 cm^{-1},[5] 31456.6 cm^{-1} [16]). All observed peaks can be assigned to vibronic bands by a comparison with MATI spectra as will be described below. For the frequency positions, see Table 1. We found no spectral features for the cis rotamer. This we attribute to the efficient cooling conditions in the nozzle leading to a very small population of the cis rotamer with a 220 cm^{-1} higher energy.

We recorded five threshold ion spectra of 1NP with the first laser frequency fixed to the 0^0_0, 49^1_0, 35^1_0, 34^1_0, and 33^1_0 bands in the $S_1 \leftarrow S_0$ transition, respectively. The five spectra shown in Figure 2 display different band structure and are displayed on a common energy scale. The zero energy level corresponds to the adiabatic ionization energy (AIE) of 1NP and results from the spectroscopic assignment of the MATI spectra in Figure 2. It is 62640 ± 5 cm^{-1} and given by the position of the cationic ground state (0^0). Within the error bars, this is in accordance with the value obtained by ZEKE spectroscopy (62637 cm^{-1}) in ref 18.

Assignment of vibrational bands in the $S_1 \leftarrow S_0$ spectrum as well as in the threshold ion spectra taken via selected intermediate states are found not only by matching the calculated energies with experimental ones. In addition, we compared similarities in the typical displacements of the vibrational modes resulting from the ab initio calculations and were able to assign the following bands.

i. ν_{49}. The band at 209 cm^{-1} in the intermediate state S_1 corresponds to the band at 237 cm^{-1} in the ion ground state $\tilde{X}$. This we found clearly from calculated displacement patterns in S_1 and $\tilde{X}$ leading to an unambiguous assignment as ν_{49}. For the intermediate state S_1, this is in agreement with the assignment in ref 20.

ii. ν_{35}. The band at 275 cm^{-1} in S_1 corresponds to the band at 282 cm^{-1} in the $\tilde{X}$. The previous assignment of ref 20 of the 275 cm^{-1} band in S_1 as the 48^1_0 transition is not corroborated by our ab initio results. The ν_{48} mode in S_1 has a strong contribution of an O−H stretching vibration, and our calculations show that the corresponding mode in the cationic ground state ($\tilde{X}$:ν_{45}) would have a more than 2-fold higher vibrational energy. This is not observed in the MATI spectrum. A better agreement of the calculated vibrational frequency in the S_1 state and the cationic ground state is given by the ν_{35} mode with in-plane character.

iii. ν_{33} and ν_{34}. According to our calculations, both the bands at 411 cm^{-1} and at 454 cm^{-1} in the S_1 state correspond to either of the two bands at 445 cm^{-1} and 460 cm^{-1} in the ionic state $\tilde{X}$. Both cationic states v_{33}' and v_{34}' are linear combinations of at least the two S_1 state levels v_{33}'' and v_{34}'': $|v_{33}' = 1\rangle = a^{33}{}_{33}|v_{33}'' = 1\rangle + a^{34}{}_{33}|v_{34}'' = 1\rangle$ and $|v_{34}' = 1\rangle = a^{33}{}_{34}|v_{33}'' = 1\rangle + a^{34}{}_{34}|v_{34}'' = 1\rangle$ (Here, the lower index denotes the initial vibrational mode, the index on top the final mode of the transition from the S_1 to the $\tilde{X}$ state: $\nu^{\text{final}}_{\text{inital}}$). The theoretical results for the square of the coefficients $a^{33}{}_{33}$, $a^{34}{}_{33}$ starting from the 33^1_0 intermediate state and $a^{33}{}_{34}$, $a^{34}{}_{34}$ starting from the 34^1_0 intermediate are given as bars in Figure 3 (right side). There are other modes mixed in but only with much lower intensity and we find a clear indication for Duschinsky rotation from theory. The experimental intensities in the MATI spectra measurement via the 33^1_0 and 34^1_0 intermediate states (Figure 3, left side) show the theoretically predicted inversion of the intensities of adjacent 34^1 and 33^1 vibrational peaks. We therefore assign the pair S_1:411 cm^{-1}/$\tilde{X}$:445 cm^{-1} to the ν_{34} mode and the pair S_1:454 cm^{-1}/$\tilde{X}$:460 cm^{-1} to the ν_{33} mode. Another mechanism which has to be considered to explain the observed mixing of the ν_{33} and ν_{34} modes is anharmonic coupling between both vibrational states separated by only 15 cm^{-1} in the cation. Here, experiments with deuterated naphthol would be useful. Because of the good agreement of our harmonic calculation, we believe that Duschinsky rotation is the main mechanism leading to the mode mixing. The assignment of ν_{34} in the S_1 state also agrees with the assignment in ref 20. From the rotationally resolved spectrum of the 411 cm^{-1}

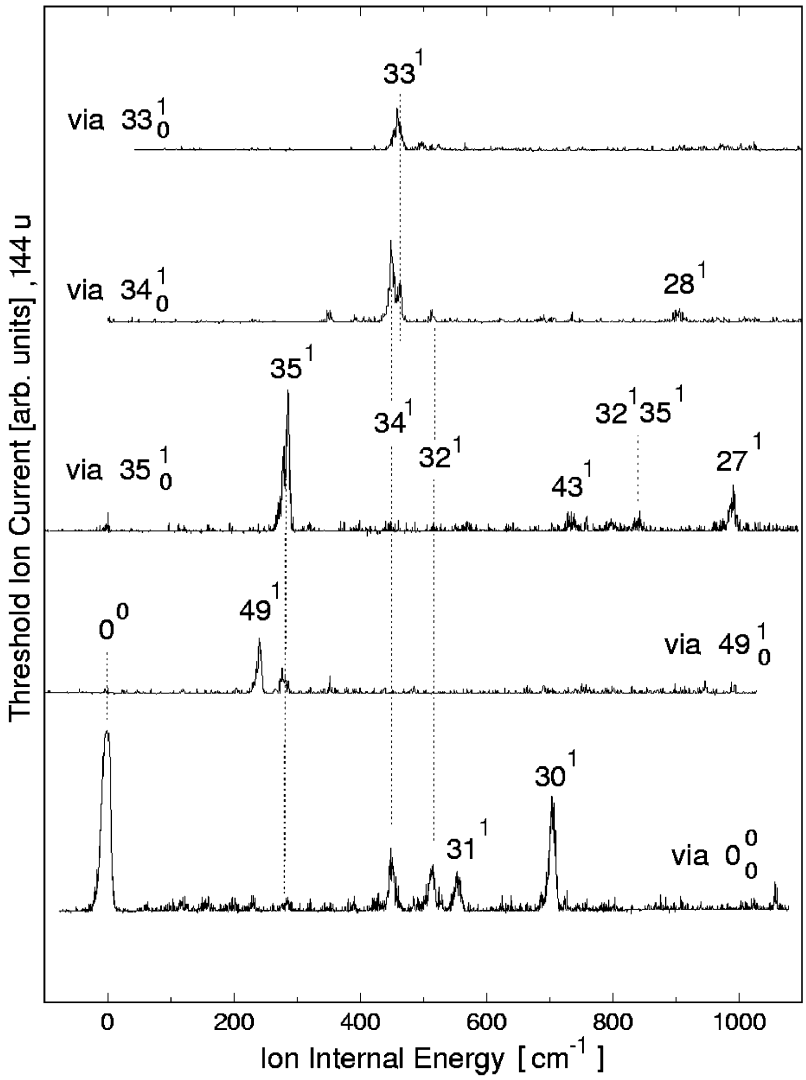

Figure 2. Threshold ion (MATI) spectra of *trans*-1-naphthol measured by resonance-enhanced two-photon excitation via the five different intermediate states indicated for each trace. For explanation of the band assignments, see text.

band in the $S_1 \leftarrow S_0$ spectrum, Humphrey and Pratt concluded (ref 31) that this mode most likely is an in-plane vibration in agreement with the displacement patterns found in our work. The relatively high difference of our theoretical result (443 cm^{-1}) for the ν_{34} frequency in S_1 from the observed one we attribute to a coupling of the mode to the S_2 state as claimed in ref 31. The calculated frequencies in the $\tilde{X}$ state listed in Table 1 state agree nicely with the experimental values.

iv. ν_{46}. The band at 415 cm^{-1} in the S_1 is separated by 4 cm^{-1} only from the 34^1_0 (411 cm^{-1}) band. Its assignment is not completely clear. An assignment as the out-of-plane 46^1_0 band is corroborated by the high-resolution experimental results of ref 31 identifying this band as a vibration with out-of-plane character because of its negative inertial defect. On the other hand, it is also possible to assign the band alternatively to the ν_{33} in-plane vibration when regarding the calculated coefficients of the displacement patterns of the ν_{34} and the ν_{33} modes in the electronic states S_0 and S_1. This would lead to a better agreement with fluorescence emission spectra of Knochenmuss et al.[12]

trans-1-Naphthol·H_2O. *trans-1-Naphthol·H_2O: REMPI.* For basic information on the solvation behavior of 1NP, we performed REMPI and MATI experiments on 1NP·H_2O clusters. The $S_1 \leftarrow S_0$ REMPI spectrum of the *trans*-1NP·H_2O shown in the lower trace of Figure 1 was obtained by averaging several individual scans. The 0^0_0 transition is located at 31313.5 cm^{-1} in good agreement with previous experiments,[8,9,32,33] shifted by 142.5 cm^{-1} to the red of the monomer. For the assignment of the vibronic bands in the $S_1 \leftarrow S_0$ spectrum, we measured three MATI spectra of 1NP·H_2O via three different intermediate states. Furthermore, the cluster assignments are corroborated by the comparison of the calculated nuclear displacement patterns of the corresponding S_1 vibrational excitations of monomer and cluster. In Figure 1, the 0^0_0 origin of both the monomer and the cluster spectra are taken as the zero point of the energy scale, so that the position of the various intramolecular bands can be directly compared. The vibrational energies are shifted only slightly because of the clustering process and most of the bands in the 1NP·H_2O spectrum can be directly found in the 1NP monomer spectrum. Only the 46^1_0 band close to the 34^1_0 band in the $S_1 \leftarrow S_0$ spectrum of the 1NP monomer has no counterpart at this position in the $S_1 \leftarrow S_0$ spectrum of the 1NP·H_2O cluster. There is a small additional band close to the 32^1_0 band we assign to the 46^1_0 band shifted to higher energy by 80 cm^{-1} in the cluster (in ref 13, the 46^1_0 transition in the monomer was assigned to the combination band $49^1_0 35^1_0$). Humphrey and Pratt stated a coupling of the band at 414 cm^{-1} to the S_2 electronic state[31] (see also ref 13). We conclude that the different frequency of the 46^1_0 band in the cluster is due to a different coupling to the S_2 state in 1NP·H_2O compared to that in the monomer.

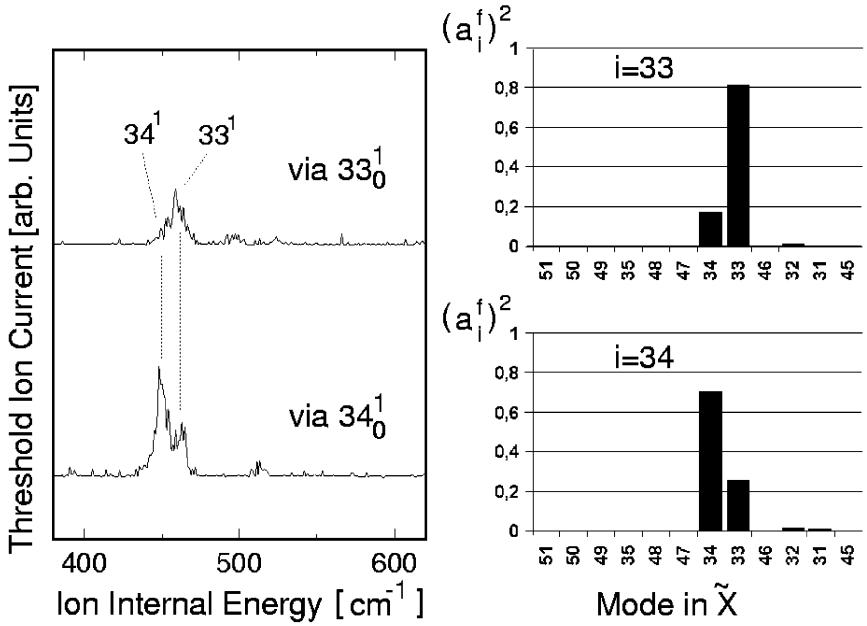

Figure 3. Left: Threshold ion spectra of *trans*-1-naphthol via the 33^1_0 (upper trace) and 34^1_0 (lower trace) intermediate states. Right: Intensities of the respective transitions calculated from the displacement patterns.

In the magnified inset of the lower trace of Figure 1, two bands at 56.2 cm^{-1} and 59.9 cm^{-1} are shown. The first transition (56.2 cm^{-1}) is assigned to the first quantum of an intermolecular in-plane bending vibration $(\beta_{ip})^1_0$, the second (59.9 cm^{-1}) is the second quantum of an out-of-plane bending vibration $(\beta_{oop})^2_0$.[13] The in-plane bending vibration is also observed as a progression of the 34^1_0 transition ($34^1_0(\beta_{ip})^1_0$) partly overlapping with the 33^1_0 transition. We found no evidence for further intermolecular vibrations in the $S_1 \leftarrow S_0$ spectrum. In particular, the stretching intermolecular vibration is not observed pointing to a small structural change of the hydrogen bonding from the S_0 to the S_1 state.

(trans-1-Naphthol·H_2O)$^+$: MATI. We recorded three threshold ion spectra, with the first laser frequency fixed to the 0^0_0, 35^1_0, and the 34^1_0 intermediate state transitions, respectively. All three spectra are shown in Figure 4 on a common ion internal energy scale, allowing for direct comparison.

In our experiments, the adiabatic ionization energy (AIE) was found at 59138 ± 10 cm^{-1}. This agrees with the value of 59000 ± 200 cm^{-1} from two-color REMPI experiments[9] but is more accurate because of the exclusive detection of threshold ions. Thus, the microsolvation of 1NP with one water molecule reduces the adiabatic ionization energy (AIE) by 3502 cm^{-1}. There are a large number of progressions of the stretching intermolecular vibration σ built on several intramolecular modes. This results from a strong increase of the intermolecular binding energy after ionization (demonstrated by the large redshift of the AIE) causing a shortening of the intermolecular distance and producing larger Franck−Condon factors for transitions with $\Delta\nu \neq 0$.

Most of the bands were assigned on the basis of our ab initio results. Using the propensity rule $\Delta\nu = 0$ for the intramolecular vibrations during the ionization process, the 34^1 and 35^1 vibrations can be easily assigned in the threshold ion spectrum of 1NP·H_2O. It is interesting to see that the intensities of most of the intramolecular vibrations in the threshold ion spectrum of the 1NP·H_2O cluster differ from the ones in the monomer. In particular, the 33^1 band appears in the threshold spectrum of the cluster measured via the 35^1_0 band but is not observed in the monomer ion spectrum. This goes in line with a frequency shift of 30 cm^{-1}. A similar situation is observed for the 35^1 band appearing as a strong band in the cluster ion spectrum but being very weak in the monomer ion spectrum. We conclude that these intensitiy changes reflect the structural changes of the molecule during the clustering process. Indeed, this is shown by a comparison of the calculated displacement patterns of the vibrations before and after the attachment of the water molecule to 1NP. All transition frequencies and their intensities are listed in Table 1.

In recent work, we measured the dissociation threshold of aromat−water clusters such as indole·H_2O and phenol·H_2O with the MATI technique.[34,35] This is based on the measurement of threshold ions at the parent and the daughter mass simultaneously.[36] A breakdown of the parent signal is observed at the dissociation threshold and at the same time an onset of the signal at the fragment (monomer) mass. This type of measurement was not possible for 1NP·H_2O because of a very high current of promptly produced ions. However, using the value of 59138 cm^{-1} for the AIE of the 1NP·H_2O cluster measured in this work for the first time in combination with the binding energy (D_0) measured by Bürgi et al. for the neutral ground-state S_0 of 2035 ± 69 cm^{-1},[33] the binding energy E_0 in the ionic states $\tilde{X}$ can be calculated from a thermochemical cycle: $E_0 = D_0 + \text{AIE}(1\text{NP}) - \text{AIE}(1\text{NP}\cdot H_2O) = 5547 \pm 75$ cm^{-1}. It is interesting to compare this value with the ones of other hydrogen-bonded systems. The value E_0 for the 1NP·H_2O cluster is considerably higher than the value measured for the indole$^+$·H_2O cation cluster (4790 ± 10 cm^{-1}). This is in line with the general rule found in solution that an O−H···O bond is stronger than an N−H···O bond. On the other hand, the binding energy of the phenol$^+$·H_2O complex measured in our recent work is 6520 cm^{-1} [35] and somewhat larger than that of 1NP·H_2O. This is explained by the more delocalized charge in the 1NP$^+$·H_2O leading to a smaller charge-induced contribution to the binding energy.

Concluding Remarks

It is interesting to compare the experimental values for the AIE and the binding energies of the neutral 1NP·H_2O and the ionic 1NP$^+$·H_2O cluster with the results from our ab initio

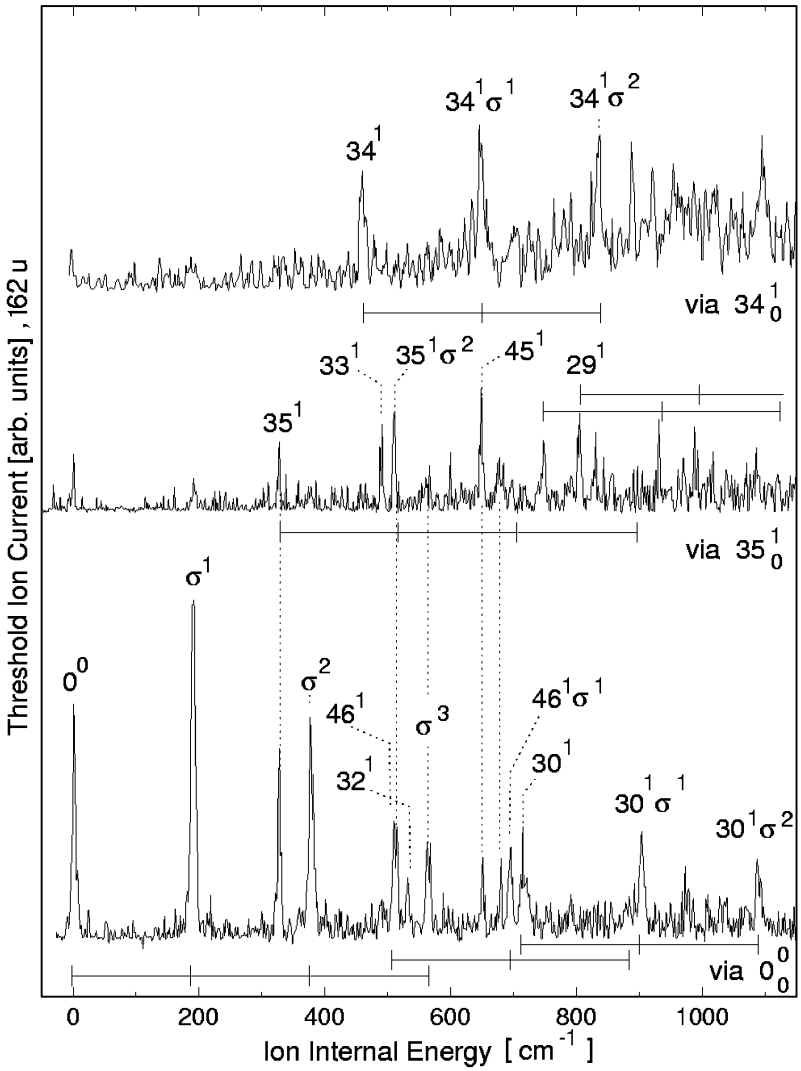

Figure 4. Threshold ion (MATI) spectra of *trans*-1-naphthol·H_2O measured by resonance-enhanced two-photon excitation via the three different intermediate states indicated for each trace. For explanation of the band assignments, see text.

calculation. This yields some information on the quality of the theoretical results used in the preceding section for the assignment of vibrational bands. The calculated AIE of 1NP·H_2O is larger by only 3.7% than the experimental value and thus is in reasonable agreement with experimental value. For the calculated binding energy, however, a much larger variance is found. It is 11.2% for the larger binding energy in the ion and 25.7% for the nearly 3 times smaller binding energy in the neutral 1NP·H_2O. This reflects the general problem with the calculation of intermolecular binding energies as a small size value resulting as the difference of large energy values with uncertainties. While the quality of the calculation of this work is sufficient to reproduce the intramolecular energies and the resulting intramolecular vibrational frequency, calculations at a much higher level are desirable for describing the energies of intermolecular bonding of clusters of polyatomic molecules. This has been demonstrated by us only recently for the indole·benzene system.[37]

In conclusion, we have shown that the combination of REMPI, threshold ionization (MATI) spectra, and ab initio calculation is very useful to investigate the solvation behavior of aromatic molecules with H_2O. We demonstrated for 1NP·H_2O that an assignment of various inter- and intramolecular bands is achieved in this way leading to a more complete picture of the structure and energetics of the cluster, both important information for an understanding of the enhanced charge-transfer process in the S_1 state.

Acknowledgment. We are grateful to Prof. Charles Parmenter for many stimulating and fruitful discussions on molecular dynamic problems during a quarter of century. The authors wish to thank Thomas Mehnert for performing ab initio calculations. Financial support from the Deutsche Forschungsgemeinschaft and the Fonds der Chemischen Industrie is gratefully acknowledged.

References and Notes

(1) Förster, Th. *Z. Elektrochem.* **1950**, *54*, 531.
(2) Weller, A. *Z. Elektrochem.* **1952**, *56*, 662.
(3) Webb, S. P.; Philips, L. A.; Yeh, S. W.; Tolbert, L. M.; Clark, J. H. *J. Phys. Chem.* **1986**, *90*, 5154.
(4) Solntsev, K. M.; Huppert, D.; Agmon, N. *J. Phys. Chem. A* **1998**, *102*, 9599.
(5) Cheshnovsky, O.; Leutwyler, S. *Chem. Phys. Lett.* **1985**, *121*, 1.
(6) Knochenmuss, R.; Cheshnovsky, O.; Leutwyler, S. *Chem. Phys. Lett.* **1988**, *144*, 317.
(7) Cheshnovsky, O.; Leutwyler, S. *J. Chem. Phys.* **1988**, *88*, 4127.
(8) Knochenmuss, R.; Leutwyler, S. *J. Chem. Phys.* **1989**, *91*, 1268.
(9) Kim, S. K.; Li, S.; Bernstein, E. R. *J. Chem. Phys.* **1991**, *95*, 3119.
(10) Knochenmuss, R. D.; Smith, D. E. *J. Chem. Phys.* **1994**, *101*, 7327.
(11) Kim, S. K.; Breen, J. J.; Willberg, D. M.; Peng, L. W.; Heikal, A.; Syage, J. A.; Zewail, A. H. *J. Phys. Chem.* **1995**, *99*, 7421.

(12) Knochenmuss, R.; Muino, P. L.; Wickleder, C. *J. Phys. Chem.* **1996**, *100*, 11218.
(13) Knochenmuss, R.; Karbach, V.; Wickleder, C.; Graf, S.; Leutwyler, S. *J. Phys. Chem. A* **1998**, *102*, 1935.
(14) Henseler, D.; Tanner, Ch.; Frey, H.-M.; Leutwyler, S. *J. Chem. Phys.* **2001**, *115*, 4055.
(15) Wickleder, C.; Henseler, D.; Leutwyler, S. *J. Chem. Phys.* **2002**, *116*, 1850.
(16) Hollas, J. M.; Thakur, S. N. *Mol. Phys.* **1974**, *27*, 1001.
(17) Hollas, J. M.; bin Hussein, M. Z. *J. Mol. Spectrosc.* **1988**, *127*, 497.
(18) Lakshminarayan, C.; Smith, J. M.; Knee, J. L. *Chem. Phys. Lett.* **1991**, *182*, 656.
(19) Johnson, J. R.; Jordan, K. D.; Plusquellic, D. F.; Pratt, D. W. *J. Chem. Phys.* **1990**, *93*, 2258.
(20) Lakshminarayan, C.; Knee, J. L. *J. Phys. Chem.* **1990**, *94*, 2637.
(21) Harris, C. M.; Selinger, B. K. *J. Phys. Chem.* **1980**, *84*, 1366.
(22) Brucker, G. A.; Kelley, D. F. *Chem. Phys.* **1989**, *136*, 213.
(23) Grebner, Th. L.; Neusser, H. J. *Chem. Phys. Lett.* **1995**, *245*, 578.
(24) Braun, J. E.; Neusser, H. J. *Mass Spectrom. Rev.* **2002**, *21*, 16.
(25) Mamyrin, B. A.; Karataev, V. I.; Shmikk, D. V.; Zagulin, V. A. *Sov. Phys. JETP* **1973**, *37*, 45.
(26) Ernstberger, B.; Krause, H.; Kiermeier, A.; Neusser, H. J. *J. Chem. Phys.* **1990**, *92*, 5285.
(27) Frisch, M. J.; Trucks, G. W.; Schlegel, H. B.; Gill, P. M. W.; Johnson, B. G.; Robb, M. A.; Cheeseman, J. R.; Keith, T.; Petersson, G. A.; Montgomery, J. A.; Raghavachari, K.; Al-Laham, M. A.; Zakrzewski, V. G.; Ortiz, J. V.; Foresman, J. B.; Cioslowski, J.; Stefanov, B. B.; Nanayakkara, A.; Challacombe, M.; Peng, C. Y.; Ayala, P. Y.; Chen, W.; Wong, M. W.; Andres, J. L.; Replogle, E. S.; Gomperts, R.; Martin, R. L.; Fox, D. J.; Binkley, J. S.; Defrees, D. J.; Baker, J.; Stewart, J. P.; Head-Gordon, M.; Gonzalez, C.; Pople, J. A. Gaussian Inc.: Pittsburgh, PA, 1995.
(28) Duschinsky, F. *Acta Physiochem. U.R.S.S.* **1937**, *1*, 551.
(29) Fujimaki, E.; Matsumoto, Y.; Fujii, A.; Ebata, T.; Mikami, N. *J. Phys. Chem. A* **2000**, *104*, 7227.
(30) Mulliken, R. *J. Chem. Phys.* **1955**, *23*, 1997.
(31) Humphrey, S. J.; Pratt, D. W. *Chem. Phys. Lett.* **1996**, *257*, 169.
(32) Yoshino, R.; Hashimoto, K.; Omi, T.; Ishiuchi, S.-i.; Fujii, M. *J. Phys. Chem. A* **1998**, *102*, 6227.
(33) Bürgi, T.; Droz, T.; Leutwyler, S. *Chem. Phys. Lett.* **1995**, *246*, 291.
(34) Braun, J. E.; Grebner, Th. L.; Neusser, H. J. *J. Phys. Chem. A* **1998**, *102*, 3273.
(35) Braun, J. E.; Mehnert, T.; Neusser, H. J. *Int. J. Mass. Spectrom.* **2000**, *203*, 1.
(36) Krause, H.; Neusser, H. J. *J. Chem. Phys.* **1993**, *99*, 6278.
(37) Braun, J. E.; Neusser, H. J.; Hobza, P. *J. Phys. Chem. A* **2003**, *107*, 3918.